Crystal structure and its correlation to intrinsic and extrinsic magnetic properties of epitaxial hard magnetic Pr-Co films

A. K. Patra,[1,2] V. Neu,[1,2] S. Fähler,[1,2] R. Groetzschel,[3] S. Bedanta,[4] W. Kleemann,[4] and L. Schultz[1,2]
[1]*IFW Dresden, Institute for Metallic Materials, P.O. Box 270116, 01171 Dresden, Germany*
[2]*Institute for Solid State Physics, Department of Physics, Dresden University of Technology, 01062 Dresden, Germany*
[3]*Institute of Ion Beam Physics and Materials Research, Forschungszentrum Dresden, P.O. Box 510119, 01314 Dresden, Germany*
[4]*Angewandte Physik, Universität Duisburg-Essen, D-47048 Duisburg, Germany*
(Received 22 December 2006; published 17 May 2007)

Pulsed laser deposited epitaxial Pr_xCo_{100-x} (x=8.7–27.6 at. %) thin films were systematically studied as a function of Pr content. Structural and magnetic measurements reveal different phases for specific composition ranges. In some cases, the phases observed are in contrast to their bulk counterparts. Uniaxial anisotropy at room temperature is observed in all the films enabling excellent hard magnetic properties. Polarization decreases monotonically with the increase of Pr content, whereas coercivity exhibits a broad maximum near the highly anisotropic $PrCo_5$ composition. For the optimum combination of coercivity and polarization, the measured $(BH)_{max}$ reaches values of 310 kJ/m^3, which exceeds the highest-energy product value reported for RE-Co (RE=rare-earth) systems. Temperature-dependent ac susceptibility measurements reveal that films with x=8.7–20.4 undergo a spin reorientation from easy axis to easy cone, but films with x=22.9–27.6 maintain their uniaxial anisotropy throughout the temperature range of investigation. From the comparison of the structural investigations and the spin reorientation temperature measurements, it is concluded that the spin reorientation temperature is insensitive to the change in the lattice parameter of the $PrCo_{5\pm\delta}$ phase.

DOI: 10.1103/PhysRevB.75.184417 PACS number(s): 75.70.Ak, 75.30.Gw, 75.50.Vv, 81.15.Fg

I. INTRODUCTION

Permanent magnet thin films are of large interest in fundamental magnetism research and are important components in today's technical thin-film applications, such as magnetic microelectromechanical systems and high-density magnetic recording. Among the family of intermetallics, RCo_5 phases have attracted much attention due to outstanding intrinsic properties such as high-ordering temperature (T_C), high magnetocrystalline anisotropy, and high saturation polarization (J_S). $PrCo_5$ possesses the largest magnetocrystalline anisotropy (~8 MJ/m^3) (Ref. 1) of all Pr-Co phases and highest theoretical energy product of all equilibrium RE-Co phases. From this theoretical viewpoint, the slightly higher saturation polarization makes $PrCo_5$ superior to the well established isostructural $SmCo_5$ for applications. However, it has hardly been exploited as bulk or thin-film magnet as it is difficult to avoid the formation of low anisotropic Pr_2Co_{17} and Pr_5Co_{19} as impurity phases.[2,3] An additional fundamental interest arises from a spin reorientation transition (SRT), which occurs at about 110 K and is apparent as an opening of the easy magnetization axis into an easy cone around the crystallographic c axis.[4,5]

Preliminary results indicate that in epitaxial films, the formation of a metastable $PrCo_7$ phase is possible at 13 at. % Pr,[6] resulting in a high-energy product of 277 kJ/m^3. In this paper, a broad composition range of epitaxial films is examined in order to understand their phase formation range, examine their intrinsic magnetic properties, and correlate them with the extrinsic properties. From Sm-Co films,[7,8] it is known that these properties can significantly differ from the bulk. Therefore, first, the properties of bulk Pr-Co (Ref. 9) and polycrystalline Pr-Co films[10] are reviewed.

Several intermetallic compounds (Pr_2Co_{17}, $PrCo_5$, and Pr_2Co_7) exist in the composition range from 8 to 28 at. % Pr. The Pr_2Co_{17} crystallizes in the rhombohedral Pr_2Co_{17} phase (Th_2Zn_{17} type) and is ferromagnetic with a Curie temperature (T_C) of 1170 K, a saturation polarization J_S=1.38 T, and an anisotropy field $\mu_0 H_A$=3.8 T and exhibits a planar anisotropy at room temperature.[1,11] $PrCo_5$ is characterized by a hexagonal $CaCu_5$-type crystal structure and the intrinsic magnetic properties are T_C=905 K, J_S=1.24 T, and $\mu_0 H_A$ =14.5 T, having uniaxial anisotropy at room temperature.[1,4,5] Pr_2Co_7 crystallizes in the hexagonal Ce_2Ni_7 structure and its known magnetic properties are T_C=620 K and $\mu_0 H_A$=10 T.[1] Necessarily, the properties of Pr-Co permanent magnets with varying Pr content will not only depend on the microstructure but also on the contribution of the different phases and their individual intrinsic properties. Chen *et al.* reported the effect of composition on the magnetic properties of mechanically milled powder and found that a uniform nanoscale microstructure and a high anisotropy field promote magnetic hardening.[9] Although a high coercivity is observed, the energy density is low because of the low remanent polarization of these isotropic magnets. Terada *et al.* investigated the effect of composition on the microstructure and magnetic properties of polycrystalline Pr-Co films as a function of rare-earth content from 0 to 20 at. %.[10] These Pr-Co films (prepared at a substrate temperature above 300 °C) have a good squareness ratio (J_R/J_S) of 0.8. However, a significant energy density is not expected because of the low coercivity in these films.

The successful preparation of epitaxial Pr-Co films[12,13] leads to samples with a defined orientation of the crystallites and therefore allows the study of the intrinsic properties without the need for single crystals. Especially, there are no reports on properties of epitaxial Pr-Co films with a varying content of rare earth. Expecting the benefit from the epitaxial growth, this paper gives a detailed investigation of structural

and magnetic (intrinsic and extrinsic) properties of epitaxial films in the composition range from 8.7 to 27.6 at. % Pr.

II. EXPERIMENT

Epitaxial Pr-Co films with Pr content ranging from 8.7 to 27.6 at. % were prepared on Cr buffered MgO(110) single-crystal substrates in an UHV pulsed laser deposition system (Lambda Physik LPX305 KrF excimer laser, 248 nm, 25 ns, $\sim 10^{-9}$ mbar) at a constant energy of 100 mJ, utilizing computer controlled target and substrate movement. The Pr-Co layer was deposited at a pulse repetition rate of 5 Hz, whereas for Cr buffer and Ta cover layer, a repetition rate of 9 Hz was used. Prior to the film deposition, rate measurements were performed on each target at room temperature using an Inficon XTM/2 rate monitor. Film thickness and composition were adjusted by varying the number of pulses on each elemental target. The Pr-Co film, the Cr buffer, and the Ta oxidation protection layer were deposited at 450, 350, and <180 °C heater temperatures, respectively. The temperature was achieved by placing a radiation heater 5 mm away from the backside of the substrate and was controlled by a thermocouple attached to the heater. The temperature at the substrate is estimated to be ~ 30 K less than the heater temperature.

In order to verify the composition and thickness of the films, two experimental techniques were employed: (i) Energy dispersive x-ray (EDX) analysis was performed using a scanning electron microscope (Philips XL20) at different acceleration voltages in combination with elemental standards and analyzed by a thin-film software.[14] (ii) Rutherford backscattering spectrometry (RBS) using 1.7 MeV $4He^+$ ions was used for standard-free thickness and composition determination on selected films. Crystallinity of the films was checked by measuring θ-2θ x-ray-diffraction (XRD) patterns in Bragg-Brentano geometry using Co $K\alpha$ radiation. To determine the texture and the phases present in the sample, partial pole figures and θ-2θ scan were measured with a Philips X'pert texture goniometer with Cu $K\alpha$ radiation. Magnetic hysteresis at room temperature was measured using a Quantum Design physical properties measurement system with vibrating-sample magnetometer (VSM) in a maximum field of 9 T. Temperature-dependent ac susceptibility was measured with an ac amplitude $\mu_0 H = 0.4$ mT and a frequency $f = 1$ Hz, by using a superconducting quantum interference device magnetometer (MPMS-5S, Quantum Design). The value of the spin reorientation transition temperature T_{SR} was evaluated from the peak of the ac susceptibility versus temperature plot.

III. RESULTS AND DISCUSSION

A. Chemical characterization

Figure 1 shows the RBS spectrum of a Pr-Co film grown on MgO(110) substrate with a Cr buffer and Ta cover layer. The solid line represents the spectrum simulated by SIMNRA 6.0 (Ref. 15) assuming a Pr-Co layer of homogeneous composition over depth, while the symbols represent the experimental data. The spectrum shows well separated peaks of all four elements present in the layer stack. The heavy Ta was intentionally chosen as cover layer to avoid overlapping of the RBS signal of the cap layer with other peaks. The measured data fit very well with the simulated spectrum. The atomic compositions and film thicknesses obtained through RBS and EDX analysis for three representative Pr-Co films are summarized in Table I. The samples are labeled with the composition obtained from the EDX analysis. Thicknesses obtained from RBS analysis for $Pr_{13}Co_{87}$ and $Pr_{17.5}Co_{82.5}$ films are in excellent agreement with the EDX measurements, although these are two independent techniques. As both methods quantify the deposited mass, lattice constants obtained from the structural investigation (see Sec. III B) were used to convert mass into thickness. For the $Pr_{27.5}Co_{72.5}$ film, the EDX analysis gives a somewhat higher value compared to RBS data. To give a lower estimate, in the case of slightly disagreeing results, always the larger thickness was used to calculate the film polarization value in unit of teslas. Compositions measured by EDX are slightly higher than the RBS values for all the films listed in Table I. However, to be consistent throughout the composition series, only the EDX results were taken for data analysis, as these measurements could easily be performed on all samples and proved to be sufficiently accurate.

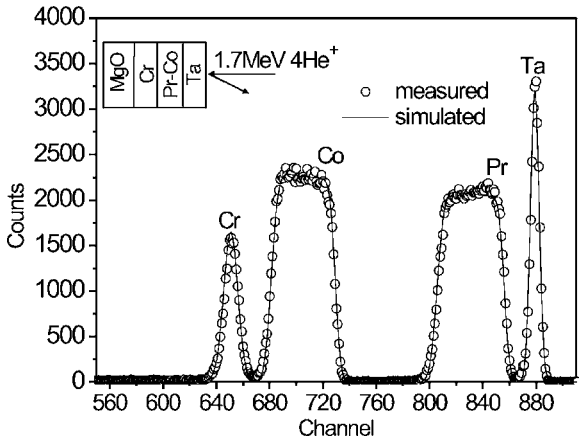

FIG. 1. RBS spectra of a $Pr_{17.5}Co_{82.5}$ film with Cr buffer and Ta cover layer.

B. Structural characterization

Shown in Fig. 2 are the XRD patterns of the Pr-Co films listed in Table I, deposited on Cr buffered MgO(110). The

TABLE I. Thickness and composition of three Pr-Co films obtained from RBS and EDX analysis. The samples are labeled with the composition obtained from the EDX analysis.

	Thickness (nm) Pr-Co layer		Composition Pr (at. %)	
Sample	RBS	EDX	RBS	EDX
$Pr_{13}Co_{87}$	71	70	11.6	13.0
$Pr_{17.5}Co_{82.5}$	83	83	16.7	17.5
$Pr_{27.5}Co_{72.5}$	86	92	27.0	27.5

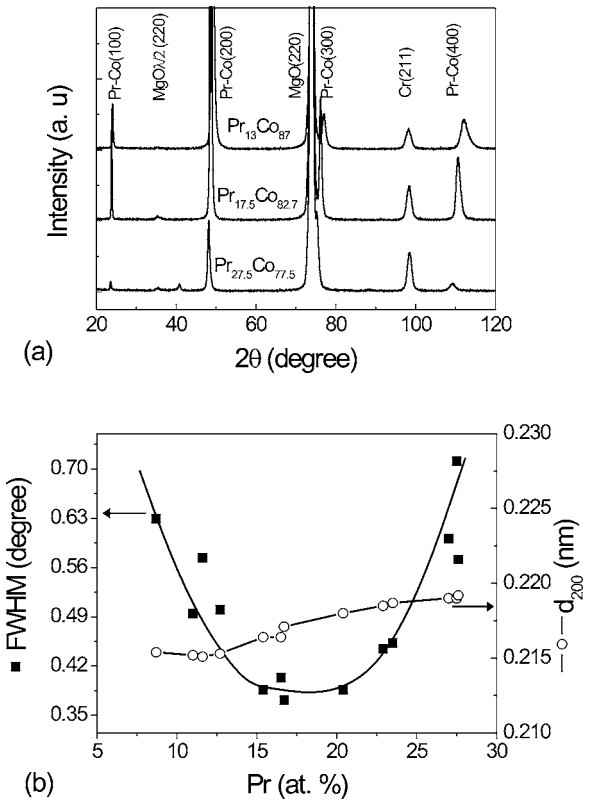

FIG. 2. (a) XRD pattern of three Pr-Co films described in Table I. (b) FWHM (solid square) and d_{200} spacing (open circle) of Pr-Co films as a function of the Pr content. Solid lines are a guide to the eyes.

patterns consist of the (220) reflection of the single-crystal MgO substrate, a Cr(211) reflection of the buffer, and (h00) Pr-Co reflections. The appearance of a single series of Pr-Co reflections indicates the textured growth of the Pr-Co films. Also, the signature of the (h00) reflections illustrates that the c axis of the Pr-Co grains lies in the substrate plane irrespective of the composition. Similar film growth is reported for sputtered Sm_2Co_7 and pulsed laser deposited $SmCo_5$ films, also on Cr buffered MgO(110) substrates.[16,17]

The 2θ position of the Pr-Co(200) peak shifts monotonically from 2θ=49.14° to 2θ=48.16° going from the $Pr_{13}Co_{87}$ to the $Pr_{27.5}Co_{72.5}$ film, respectively, which indicates the formation of Pr-Co phases with a varying unit cell. The lattice spacing obtained from the measured (200) peak position of the XRD pattern increases monotonously with Pr content above 13 at. %, as shown in Fig. 2(b). The measured d_{200} value (0.2190 nm) of the $Pr_{27.5}Co_{72.5}$ film matches quite well with the expected value (0.2191 nm) of the hexagonal unit cell (Ce_2Ni_7-type structure). Similar results are observed for the $Pr_{17.5}Co_{82.5}$ film with a clear agreement between the measured value (0.2171 nm) and the value expected (0.2172 nm) for a hexagonal unit cell ($CaCu_5$-type structure). However, there is a clear disagreement between the values measured (0.2151 nm) and expected (0.2109 nm) for a rhombohedral unit cell (Th_2Zn_{17}-type structure) for $Pr_{13}Co_{87}$, a first indication that this film exhibits a different unit cell.

The line broadening of the Pr-Co(200) reflection measured by XRD as a function of Pr content is shown in Fig. 2(b). The full width at half maximum (FWHM) follows a parabolic behavior with its minimum close to the $PrCo_5$ composition and largely increases toward low (Pr_2Co_{17}) and high (Pr_2Co_7) Pr concentrations. It is known that the stable RE-Co phases in the composition range from 10 to 22 at. % RE, i.e., RE_2Co_{17}, $RECo_5$, and RE_2Co_7, differ mainly in the stacking sequence along the c axis of only a few varieties of RE and Co rich planes.[18] This explains the close similarity in the x-ray-diffraction patterns of most phases with only a slight difference in lattice parameters and only a small number of exclusive reflections. In the intermediate composition range between 10 and 17 at. % RE, the $TbCu_7$ structure holds a special position, as it is derived from the $CaCu_5$ structure by a partial replacement of RE atoms by Co dumbbells.[19] Although reported only for a given Co to RE ratio of 7 (22% replacement of RE atoms), the substitution scheme holds for a variable amount of RE atoms and thus is not clearly distinguishable from a $CaCu_{5\pm\delta}$ phase for small δ. Thus, we refer to the crystallographic arrangement of $RECo_7$ as a structure rather than a phase. A similar view is taken by Ge *et al.*,[20] who interpret this structure as $CaCu_5$ phase with extended solubility of Co. Toward a composition of RE_2Co_{17} (a 33% substitution of RE atoms), the Th_2Zn_{17} structure is clearly distinguishable as an own phase with a unique atomic arrangement. From the above consideration, it can be concluded that epitaxial films prepared with the $PrCo_5$ composition grow in a well defined crystal structure with a small variation in lattice spacing, whereas for a lower and a higher Pr content, it is suggested that the partial substitution of Co for Pr is locally rather inhomogeneous and thus leads to the observed broadening of the (200) reflection. An alternative explanation of stress originating from a varying lattice mismatch to the Cr(211) buffer is less likely, as the differences are not significant.

Pole figure measurements are a useful technique to determine the orientation relationship of the film with respect to the substrate and buffer. At the same time, these measurements can be used to identify the different phases present in the films by measuring distinct Bragg reflections.[21] This is especially necessary for epitaxial films, as the low number of lattice planes parallel to the surface make measurements in Bragg-Brentano geometry insufficient for a phase analysis. Pole figure measurements have been performed on all films with Pr content varying from 8.7 to 27.6 at. %. The measurements are discussed and interpreted exemplarily for the three samples listed in Table I. Figures 3(a), 3(d), and 3(g) show measured Pr-Co(110) quarter pole figures. The appearance of a single pole proves that the c axis of the Pr-Co grains lies along the MgO[001] substrate direction for all the samples, in agreement with the (h00) texture found in the XRD measurements. Also, other pole figure measurements (not shown here) such as for Pr-Co(101) and Pr-Co(111) poles are in perfect agreement with the above mentioned texture and are confirmed by a texture simulation software.[22] These observations imply that, irrespective of the composition, the c axis of the Pr-Co unit cell has a unique in-plane orientation. The full epitaxial relationship is Pr-Co(100)[001]$\|$Cr(211) $\times[0\ \bar{1}\ 1]\|$MgO(110)[001]. Considering the nominal composition of the Pr-Co films listed in Table I, the phases expected

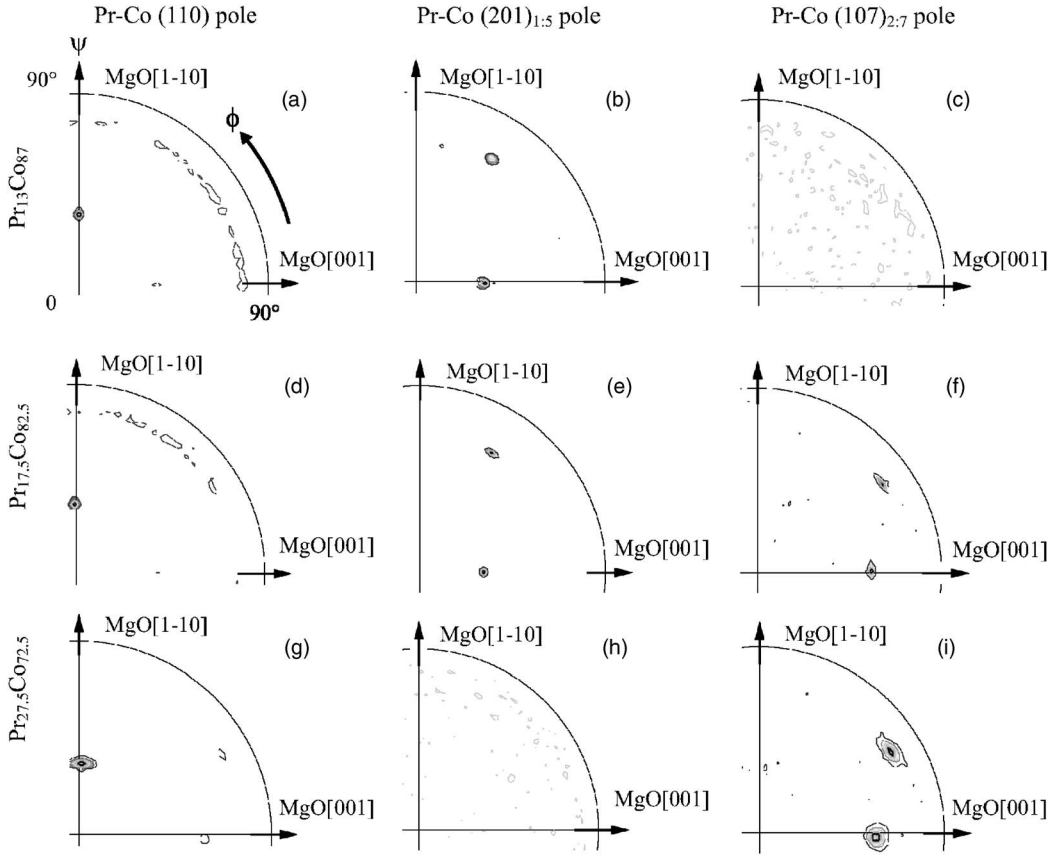

FIG. 3. Partial pole figures of $Pr_{13}Co_{87}$, $Pr_{17.5}Co_{82.5}$, and $Pr_{27.5}Co_{72.5}$ films. (a), (d), and (g) are Pr-Co(110) poles; (b), (e), and (h) are Pr-Co(201) poles; and (c), (f), and (i) are Pr-Co(107) poles. The scale of the individual pole figures is adjusted to make the relevant information more visible.

from the equilibrium phase diagram are the ordered rhombohedral Pr_2Co_{17} phase (Th_2Zn_{17} type), hexagonal $PrCo_5$ phase ($CaCu_5$ type), and the Pr_2Co_7 phase (Ce_2Ni_7 type) for the $Pr_{13}Co_{87}$, $Pr_{17.5}Co_{82.5}$, and $Pr_{27.5}Co_{72.5}$ films, respectively. The Pr-Co(110), Pr-Co(101), and Pr-Co(111) reflections described above are common reflections occurring for all three mentioned Pr-Co phases.[23] On the other hand, the Pr-Co(204), Pr-Co (201), and Pr-Co(107) reflections are distinct reflections, which exclusively occur for the Pr_2Co_{17}, $PrCo_5$, and Pr_2Co_7 phases, respectively. The characteristic Pr-Co(204) pole expected for the Pr_2Co_{17} phase is not observed in the $Pr_{13}Co_{87}$ film. Also, the maximum intensity of 10 counts measured in a Pr-Co(107) pole figure [Fig. 3(c)] rules out the presence of the Pr_2Co_7 phase in this film. On the other hand, the signature of a Pr-Co(201) pole [Fig. 3(b)] indicates that this film crystallizes in the disordered hexagonal $PrCo_7$ structure ($TbCu_7$ type) rather than in the ordered rhombohedral Pr_2Co_{17} phase. The phase identification and the precise crystal structure of this film are described in detail in Ref. 6. As expected, the $Pr_{17.5}Co_{82.5}$ film shows a clear Pr-Co(201) pole figure [shown in Fig. 3(e)], suggesting that the film crystallizes in the hexagonal $PrCo_5$ phase. However, a pole figure measurement of the Pr-Co(107) reflection [Fig. 3(f)] illustrates the additional presence of the hexagonal Pr_2Co_7 phase. This film with 17.5 at. % Pr consists of a mixture of the hard magnetic hexagonal $PrCo_5$ ($CaCu_5$-type) and Pr_2Co_7 (Ce_2Ni_7-type) phases. Figure 3(i) shows a measured Pr-Co(107) pole for the $Pr_{27.5}Co_{72.5}$ film and confirms the presence of the hexagonal Pr_2Co_7 phase. The measured Pr-Co(201) [Fig. 3(h)] and (204) poles (not shown here) show no significant reflections (maximum intensity of 10 counts) and suggest the single-phase behavior of the $Pr_{27.5}Co_{72.5}$ film.

Due to the small number of visible reflections, a complete structure determination cannot be achieved in epitaxial thin films by typical XRD measurement in Bragg-Brentano geometry. An alternative is the measurement of 2θ values of several (hkl) planes on tilted poles in a pole figure measurement setup. 2θ values of the Pr-Co(110), Pr-Co(101), Pr-Co(200), Pr-Co(201), and Pr-Co(107) reflections have been measured for the $Pr_{13}Co_{87}$, $Pr_{17.5}Co_{82.5}$, and $Pr_{27.5}Co_{72.5}$ films. In order to obtain the a and c values from the experimentally measured scans, theoretical peak positions have been calculated by a structure simulation software for different phases and the lattice parameters have been optimized to give the best agreement with the experimental data. The optimized a and c values for the Pr-Co films mentioned above are listed in Table II with the values reported for similar bulk phases. There is a clear disagreement between the measured values of the lattice parameters and the values expected for an ordered rhombohedral crystal structure for the $Pr_{13}Co_{87}$ film, as described in Ref. 6. As the disordered hexagonal $PrCo_7$ phase is not an equilibrium bulk phase, the lattice parameters of the $Pr_{13}Co_{87}$ film with disordered hexagonal $PrCo_7$ structure have been compared with a Pr-Co bulk

TABLE II. Deduced lattice parameters (a and c) of $Pr_{13}Co_{87}$, $Pr_{17.5}Co_{82.5}$, and $Pr_{27.5}Co_{72.5}$ films with the corresponding bulk values of a similar phase. The values for the $Pr_{13}Co_{87}$ film are taken from Ref. 6.

Sample		Optimized	Bulk literature
$Pr_{13}Co_{87}$	a (nm)	(0.498±0.001)	0.4924[a]
	c (nm)	(0.404±0.001)	0.4042
$Pr_{17.5}Co_{82.5}$	a (nm)	(0.501±0.001)	0.5016[b]
	c (nm)	(0.399±0.001)	0.3994
$Pr_{27.5}Co_{72.5}$	a (nm)	(0.508±0.001)	0.5061[b]
	c (nm)	(2.403±0.001)	2.4171

[a]Reference 24.
[b]Reference 9.

sample with minimum concentration of additives, for which the hexagonal $PrCo_7$ is observed. There is good agreement between the measured values of the lattice parameters with the values of mechanically milled $PrCo_{6.7}Zr_{0.3}$ powders.[24] An excellent agreement between the deduced values of the lattice parameters for the $Pr_{17.5}Co_{82.5}$ film with the values of the bulk phase is obtained. Good agreement between the measured values of the lattice parameter a and the corresponding bulk value for $Pr_{27.5}Co_{72.5}$ is observed. However, only a fair agreement is obtained for the c lattice parameter.

Though our structural investigation indicates a single-phase nature of the Pr-Co films in some composition, the presence of stacking disordered along the c axis, as observed for Sm-Co films investigated by transmission electron microscopy (TEM), cannot be ruled out.[25] Indeed, the large FWHM observed for the films apart from a $PrCo_5$ composition suggests that the lattice distance or the stacking order varies on a rather small length scale, as opposed to a mixture of phases with coherent regions large enough to result in distinguishable XRD reflections.

C. Magnetic properties

Figure 4 shows room-temperature hysteresis loops of $Pr_{13}Co_{87}$, $Pr_{17.5}Co_{82.5}$, and $Pr_{27.5}Co_{72.5}$ films measured along the three nonequivalent perpendicular directions. Largely open loops along the MgO[001] direction (parallel to c axis) represent measurements for a uniaxial hard magnet. Nearly closed loops along MgO[1-10] and MgO[110] directions are observed, as expected when measuring a highly anisotropic magnet along a hard axis. None of the hard axis curves of the above-mentioned Pr-Co films saturate at 9 T (maximum field available for the measurement), illustrating that the anisotropy field $\mu_0 H_A$ of these films is larger than 9 T. The epitaxial growth allows us to estimate the anisotropy field by extrapolating the easy and hard axis curves. From the extrapolated intersection, the anisotropy fields are estimated to be $\mu_0 H_A = 11$, 14, and 10 T for the $Pr_{13}Co_{87}$, $Pr_{17.5}Co_{82.5}$, and $Pr_{27.5}Co_{72.5}$ films, respectively, which is in excellent agreement with a bulk $PrCo_{7-x}Zr_x$ ($x=0.2$) magnet with $PrCo_7$-type structure,[26] the bulk $PrCo_5$ phase, and the Pr_2Co_7 phase.[1]

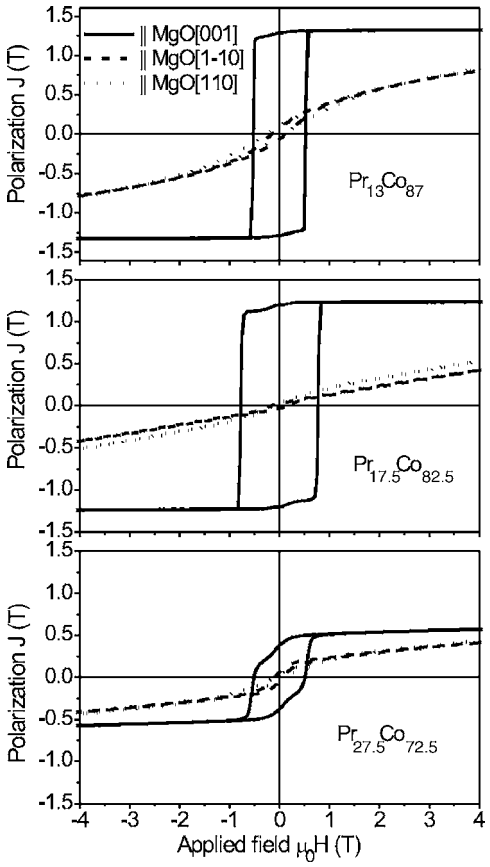

FIG. 4. Room-temperature hysteresis loops of $Pr_{13}Co_{87}$, $Pr_{17.5}Co_{82.5}$, and $Pr_{27.5}Co_{72.5}$ films measured with the field parallel to MgO[001], MgO[1-10], and MgO[110]. Curves are not desheared.

Figure 5 summarizes the magnetic properties of the Pr-Co films as a function of Pr content measured at room temperature. Shown in Fig. 5(a) are the saturation polarization (J_S) taken from the value measured at 9 T along the easy axis, the remanent polarization (J_R) measured along MgO[001], and the remanence ratio ($J_R^{\text{hard}}/J_R^{\text{easy}}$), which is taken as a measure for the magnetic texture. J_S decreases monotonously with increase of Pr content. This is understood from the dilution of the magnetic entity in the system, when replacing Co ($4.9-5.9\mu_B$) atoms by Pr ($3.5\mu_B$). The remanent polarization J_R follows the trend of J_S and decreases for higher Pr content. In the whole composition range investigated here, J_S and J_R vary from 1.51 to 0.5 T and from 1.45 to 0.29 T, respectively. As can be seen by the close match of J_R and J_S, the squareness (J_R/J_S) exhibits values close to 1 (>0.9) for most of the samples; only for the Pr rich films, it is reduced to 0.58.

The remanence ratio between the hard and the easy axis is a measure of the magnetic texture in the magnetic material. This value ranges from zero for a completely anisotropic magnet to 1 for an isotropic magnet. The observed magnetic texture smaller than 0.12 for both hard directions shows the high anisotropic nature of the Pr-Co films irrespective of composition and phase and demonstrates the advantage of epitaxial growth.

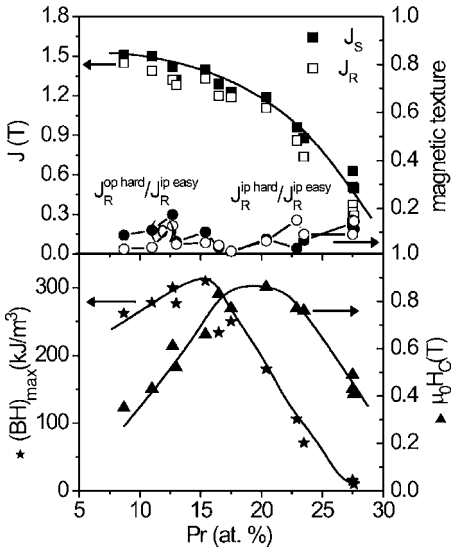

FIG. 5. Variation of the magnetic properties of Pr-Co films as a function of the Pr concentration. (a) Saturation polarization J_S (full square), remanent polarization J_R (open square), and magnetic texture (full and open circle). (b) Coercivity (full triangle) and energy density. "Ip" and "op" correspond to in plane and out of plane. Solid lines are a guide to the eyes.

Shown in Fig. 5(b) are the coercivity $\mu_0 H_C$ and the energy density $(BH)_{max}$ as a function of the rare-earth content. The coercivity reaches values between 0.35 and 0.86 T, which are rather high for epitaxially grown films, and thus have to originate from specific deviations of the microstructure from the perfect single-crystal state. A similar behavior (i.e., surprisingly high coercivity) has already been reported for isostructural, epitaxial Sm-Co films[16,17] and was discussed in terms of stacking disorder along the *c*-axis for Sm_2Co_7 films.[25] Detailed microstructural investigation by transmission electron microscopy for $PrCo_5$ films is underway but is beyond the scope of this paper. For this work, the high coercivity is considered as a general feature of these granular, epitaxial films and the focus is put on the variation of the coercivity with composition. For the film with lowest Pr content (8.7 at. %), the coercivity is $\mu_0 H_C$=0.35 T. It increases with increasing Pr content, reaches a broad maximum of $\mu_0 H_C$=0.8 T around 16.5–23.5 at. % Pr, and decreases for higher Pr content. A similar trend has been reported for polycrystalline Pr-Co films with a maximum of $\mu_0 H_C$=0.4 T for 20 at. % Pr, where the $PrCo_5$ compound is formed[10] and for mechanically milled powders with a high coercivity $\mu_0 H_C$ =2.3 T for 19 at. % Pr.[9] Coercivity requires both a high anisotropy field and an appropriate microstructure. As discussed in the structural investigations, these Pr-Co films crystallize in the $PrCo_7$ structure, $PrCo_5$, and Pr_2Co_7 phase in the vicinity of their nominal composition, respectively. Among them, the $PrCo_5$ phase exhibits a maximum anisotropy field $\mu_0 H_A$ of 14 T as compared to 11 and 10 T for the $PrCo_7$ structure and the Pr_2Co_7 phase, respectively. From this consideration, one expects a maximum coercivity around the $PrCo_5$ phase, which is indeed observed [Fig. 5(b)]. The above argument is strictly valid only when a similar microstructure is obtained for all films. However, as the observed variation in coercivity follows the trend dictated by the anisotropy, we can deduce that the microstructural differences, which are discussed in Sec. III B, do not largely influence the coercivity.

In Fig. 5(b), the energy density is also plotted as a function of the Pr concentration. $(BH)_{max}$ follows a similar trend as the coercivity and reaches a maximum around 15.4 at. % Pr. The very high $(BH)_{max}$ values of 250–280 kJ/m^3 for films with 8.7–13 at. % Pr are based on the high saturation polarization achieved in these Co rich films. The energy density is limited here by the coercivity. This has been demonstrated for a film with 13 at. % Pr,[6] which obtained values of $(BH)_{max}$=277 kJ/m^3 with J_S=1.32 T, J_R=1.28 T, and $\mu_0 H_C$=0.52 T. The theoretical maximum energy density of a hard magnet with polarization J_S=1.32 T is $(BH)^{th}_{max}$ =346 kJ/m^3 but requires a coercivity $\mu_0 H_C > J_S/2$=0.66 T, which is not met by the epitaxial film. Thus, by increasing the coercivity, one expects the energy density to come closer to the theoretical upper limit. This is, indeed, observed for the films with ≈15 at. % Pr. The optimum combination of coercivity and polarization results in a high-energy density of $(BH)_{max}$=310 kJ/m^3. The reduction of $(BH)_{max}$ at low Pr content is due to the low coercivity and at higher Pr content, it is due to too low J_S. The high-energy density value of 310 kJ/m^3 obtained in this epitaxial Pr-Co film exceeds the energy density values reported for single-phase Sm-Co films,[27] multiphase Sm-Co/Co films,[28] exchange coupled epitaxial Sm-Co/Fe bilayers[29] and $SmCo_5$/Fe/$SmCo_5$ trilayers,[30] fiber textured Sm-Co/Fe multilayers,[31] and isotropic Pr-Co/Co films,[32] and they are necessarily better than the properties of less textured Pr-Co bulk[9] and thin films.[10]

D. Spin reorientation transition (SRT)

ac susceptibility is very sensitive to any type of magnetic phase transition and is often used to detect the spin reorientation transition as an anomaly in the temperature dependency. Figure 6 shows the real part of the ac susceptibility (χ') as a function of temperature for $Pr_{13}Co_{87}$, $Pr_{17.5}Co_{82.5}$, and $Pr_{27.5}Co_{72.5}$ films measured perpendicular to the *c* axis (parallel to MgO[110]). χ' increases with decreasing temperature and exhibits a maximum for the $Pr_{13}Co_{87}$ and $Pr_{17.5}Co_{82.5}$ films. This anomalous behavior in χ' vs temperature is ascribed to the SRT in these films, which is in agreement with reports on magnetic measurements on polycrystalline bulk $PrCo_{7-x}Zr_x$ (x=0.2) (Ref. 26) with $TbCu_7$-type structure, magnetic measurements on a $PrCo_5$ single crystal,[4] and ac susceptibility measurements on bulk $PrCo_5$ powder[33] with $CaCu_5$ structure, respectively. Above the spin reorientation temperature (T_{SR}), the *c* axis is the easy axis of magnetization and below this temperature, it opens into an easy cone. On the other hand, no anomaly in χ' in the experimental temperature range for the $Pr_{27.5}Co_{72.5}$ film reveals the absence of spin reorientation in this Pr-Co film with a Pr_2Co_7 phase (Ce_2Ni_7 type).

In the following, the observation of SRT is discussed together with the crystal structure and lattice dimensions obtained from the structural investigation in order to clarify possible correlations. The spin reorientation temperature

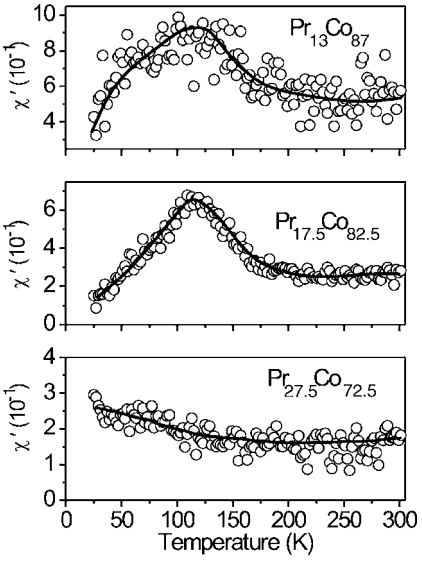

FIG. 6. Temperature dependency of ac magnetic susceptibility of $Pr_{13}Co_{87}$, $Pr_{17.5}Co_{82.5}$, and $Pr_{27.5}Co_{72.5}$ films measured perpendicular to the c axis (parallel to MgO[110]). Solid lines are a guide to the eyes.

(T_{SR}) as determined from the maximum in the χ' vs temperature curves (Fig. 6) for the series of Pr-Co films is summarized in Fig. 7 together with results from the phase analysis. Pr-Co films with $8.7 \leqslant$ Pr at. % $\leqslant 13$ crystallize in the disordered hexagonal $PrCo_7$ structure with $T_{SR} \sim 115$ K. Despite the obvious change in composition, T_{SR} as well as the values of d_{200} [Fig. 2(b)] and, therefore, the lattice parameter a are more or less constant, whereas the lattice parameter c decreases for higher Pr contents (Table II).

Films prepared in the range of $15.4 \leqslant$ Pr at. % $\leqslant 20.4$ exhibit a mixture of hexagonal $PrCo_5$ and Pr_2Co_7 phases and

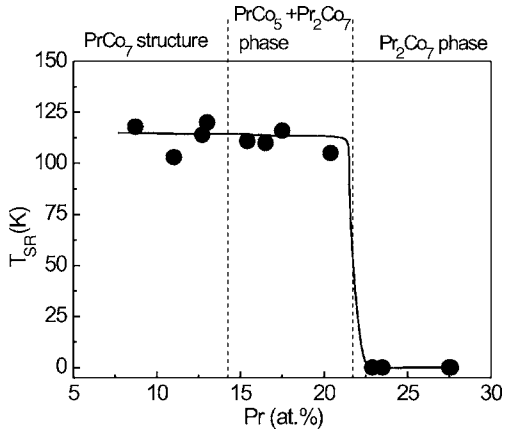

FIG. 7. Summary of SRT temperature and crystallographic phases of Pr-Co films measured as a function of Pr concentration. Solid lines are a guide to the eyes.

undergo SRT at $T_{SR} \sim 110$ K. In the same composition range, d_{200} increases with Pr concentration [Fig. 2(b)]. Pr-Co films with $22.9 <$ Pr at. % $\leqslant 27.6$ crystallize in the Pr_2Co_7 phase and preserve their uniaxial anisotropy throughout the temperature range of investigation. The d_{200} [Fig. 2(b)] continuously increases with increasing Pr content for these films, indicating a further expansion of the basal plane. Comparing the observed structural changes and the spin reorientation temperature, it is concluded that spin reorientation occurs for all the hexagonal crystal structures derived from the $CaCu_5$ structure by partial substitution of Pr or Co forming disordered structure in the composition range of 8.7–20.4 at. % Pr. Above 22 at. %, when the stoichiometric composition of the Pr_2Co_7 phase is reached, spin reorientation vanishes. The almost constant values of T_{SR} below 20.4 at. % for the $PrCo_{5\pm\delta}$ phase suggest that the T_{SR} is insensitive to the change in the lattice parameters.

IV. CONCLUSIONS

Epitaxial Pr-Co films with varying rare-earth content and with (h00) texture were deposited on Cr buffered MgO(110) single-crystal substrates by pulsed laser deposition. In the whole composition range ($8.7 \leqslant$ Pr at. % $\leqslant 27.6$), Pr-Co films grow epitaxially with a unique alignment of the c axis along the MgO[001] direction of the substrate. The dominant phases present in these films are the disordered hexagonal $PrCo_7$ structure ($TbCu_7$ type), the hexagonal $PrCo_5$ phase ($CaCu_5$ type), and the hexagonal Pr_2Co_7 phase (Ce_2Ni_7 type). Pr-Co films prepared in the range of $8.7 \leqslant$ Pr at. % $\leqslant 13$ crystallize in the disordered $PrCo_7$ structure rather than in the ordered rhombohedral Pr_2Co_{17} phase. Pr-Co films with $15.4 \leqslant$ Pr at. % $\leqslant 20.4$ exhibit a mixture of hexagonal $PrCo_5$ and Pr_2Co_7 phases. For Pr-Co films with $22.9 <$ Pr at. % $\leqslant 27.6$, a single Pr_2Co_7 phase is observed. All Pr-Co films have a uniaxial anisotropy at room temperature with an anisotropy field of $\mu_0 H_A > 9$ T. While the $Pr_{13}Co_{87}$ and $Pr_{17.5}Co_{82.5}$ films undergo a spin reorientation from the easy axis to easy cone between 120 and 105 K. Pr_2Co_7 films preserve their uniaxial anisotropy throughout the temperature range of investigation. Spin reorientation is observed for all Pr-Co films prepared in the range of 8.6–20.4 at. % Pr and structural changes together with the spin reorientation suggest that the spin reorientation temperature is insensitive to the change in the lattice parameter of the hexagonal $PrCo_{5\pm\delta}$ phase. Due to the high anisotropy field of the $PrCo_5$ phase and the excellent epitaxial growth, $PrCo_{5\pm\delta}$ films show very good magnetic properties in this series. In the optimum condition, with $\mu_0 H_C = 0.66$ T, $J_R = 1.33$ T, and squareness $= 0.95$, the measured $(BH)_{max}$ reaches 310 kJ/m^3, which is the best value reported for RE-Co magnets.

ACKNOWLEDGMENT

This work is supported by the DFG as part of the SFB 463: "Rare Earth Transition Metal Compounds: Structure, Magnetism and Transport."

[1] A. E. Ray and K. J. Strnat, IEEE Trans. Magn. **11**, 1429 (1975).
[2] W. E. Wallace, R. S. Craig, H. O. Gupta, S. Hirosawa, A. Pedziwiatr, E. Oswald, and E. Schwab, IEEE Trans. Magn. **20**, 1559 (1984).
[3] B. E. Meacham and D. J. Branagan, J. Appl. Phys. **93**, 7963 (2003).
[4] E. Tatsumoto, T. Okamoto, H. Fujii, and C. Inoue, J. Phys. (Paris) **32**, C1–550 (1971).
[5] H. P. Klein, A. Menth, and R. S. Perkins, Physica B & C **80**, 153 (1975).
[6] A. K. Patra, V. Neu, S. Fähler, R. Groetzschel, and L. Schultz, Appl. Phys. Lett. **89**, 142512 (2006).
[7] V. Neu and S. A. Shaheen, J. Appl. Phys. **86**, 7006 (1999).
[8] V. Neu, U. Hannemann, S. Fähler, B. Holzapfel, and L. Schultz, J. Appl. Phys. **91**, 8180 (2002).
[9] Z. Chen, Y. Zhang, and G. C. Hadjipanayis, J. Appl. Phys. **88**, 1547 (2000).
[10] N. Terada, M. Naoe, and Y. Hoshi, J. Appl. Phys. **57**, 4170 (1985).
[11] L. Zhang, D. C. Zeng, Y. N. Liang, J. C. P. Klaasse, E. Brück, Z. Y. Liu, F. R. de Boer, and K. H. J. Buschow, J. Alloys Compd. **302**, 5 (2000).
[12] D. J. Keavney, E. E. Fullerton, D. Li, C. H. Sowers, S. D. Bader, K. Goodman, J. G. Tobin, and R. Carr, Phys. Rev. B **57**, 5291 (1998).
[13] A. K. Patra, V. Neu, S. Fähler, H. Wendrock, and L. Schultz, J. Appl. Phys. **100**, 043905 (2006).
[14] STRATAGEM 2.7 by SAMx.
[15] M. Mayer, in Proceedings of the 15th International Conference on the Application of Accelerators in Research and Industry, AIP Conf. Proc. No. 475, edited by J. L. Duggan and I. L. Morgan (AIP, New York, 1999), p. 541.
[16] E. E. Fullerton, J. S. Jiang, C. Rehm, C. H. Sowers, S. D. Bader, J. B. Patel, and X. Z. Wu, Appl. Phys. Lett. **71**, 1579 (1997).
[17] A. Singh, V. Neu, R. Tamm, K. Rao, S. Fähler, W. Skrotzki, L. Schultz, and B. Holzapfel, J. Appl. Phys. **99**, 08E917 (2006).
[18] K. H. J. Buschow, Rep. Prog. Phys. **40**, 1179 (1977).
[19] Y. Khan, Acta Crystallogr., Sect. B: Struct. Crystallogr. Cryst. Chem. **29**, 2502 (1973).
[20] W. Q. Ge, C. H. Wu, and Y. C. Chuang, Z. Metallkd. **84**, 165 (1993).
[21] A. Singh, V. Neu, R. Tamm, K. S. Rao, S. Fähler, W. Skrotzki, L. Schultz, and B. Holzapfel, Appl. Phys. Lett. **87**, 072505 (2005).
[22] CARINE CRYSTALLOGRAPHY V3.1 by DIVERGENT S.A., France.
[23] Notations used in the text are valid for hexagonal phases. For the rhombohedral phase, crystallographic equivalent orientations have been measured [for example, (300) of the rhombohedral phase is equivalent to (110) of the hexagonal phase] but the indices are named according to the hexagonal counterpart for simplicity.
[24] Z. Chen, X. Meng-Burany, and G. C. Hadjipanayis, J. Appl. Phys. **87**, 5302 (2000).
[25] M. Benaissa, K. M. Krishnan, E. E. Fullerton, and J. S. Jiang, IEEE Trans. Magn. **34**, 1204 (1998).
[26] M. Q. Huang, M. Drennan, W. E. Wallace, M. E. McHenry, Q. Chen, and B. M. Ma, J. Appl. Phys. **85**, 5663 (1999).
[27] R. Rani, F. J. Cadieu, X. R. Qian, W. A. Mendoza, and S. A. Shaheen, J. Appl. Phys. **81**, 5634 (1997).
[28] R. Andreescu and M. J. O'Shea, J. Appl. Phys. **91**, 8183 (2002).
[29] J. S. Jiang, J. E. Pearson, Z. Y. Liu, B. Kabius, S. Trasobares, D. J. Miller, S. D. Bader, D. R. Lee, D. Haskel, G. Srajer, and J. P. Liu, Appl. Phys. Lett. **85**, 5293 (2004).
[30] V. Neu, K. Häfner, A. K. Patra, and L. Schultz, J. Phys. D **39**, 5116 (2006).
[31] J. Zhang, Y. K. Takahashi, R. Gopalan, and K. Hono, Appl. Phys. Lett. **86**, 122509 (2005).
[32] P. Liu, Y. Liu, and D. J. Sellmyer, J. Appl. Phys. **83**, 6608 (1998).
[33] P. A. Algarabel, A. Del. Moral, M. R. Ibarra, and J. I. Arnaudas, J. Phys. Chem. Solids **49**, 213 (1988).